Journal of Energy Chemistry 63 (2021) 130–137

Contents lists available at ScienceDirect

Journal of Energy Chemistry

journal homepage: www.elsevier.com/locate/jechem

http://www.journals.elsevier.com/journal-of-energy-chemistry/

Dedicated to the 100th anniversary of Chemistry at Nankai University

Gas-phase CO_2 activation with single electrons, metal atoms, clusters, and molecules

Ruijing Wang [a], Gaoxiang Liu [b], Seong Keun Kim [c], Kit H. Bowen [d], Xinxing Zhang [a,*]

[a] College of Chemistry, Key Laboratory of Advanced Energy Materials Chemistry (Ministry of Education), Renewable Energy Conversion and Storage Center (ReCAST), Frontiers Science Center for New Organic Matter, Nankai University, Tianjin 300071, China
[b] Advanced Bioimaging Center, Department of Molecular and Cell Biology, University of California, Berkeley, Berkeley, CA 94720, USA
[c] Department of Chemistry, Seoul National University, Seoul 08826, Korea
[d] Departments of Chemistry and Material Science, Johns Hopkins University, Baltimore, MD 21218, USA

ARTICLE INFO

Article history:
Received 29 May 2021
Revised 17 August 2021
Accepted 17 September 2021
Available online 25 October 2021

Keywords:
CO_2 activation
CO_2 anion
Gas-phase cluster
Electronic structure

ABSTRACT

In this review, the history and outlook of gas-phase CO_2 activation using single electrons, metal atoms, clusters (mainly metal hydride clusters), and molecules are discussed on both of the experimental and theoretical fronts. Although the development of bulk solid-state materials for the activation and conversion of CO_2 into value-added products have enjoyed great success in the past several decades, this review focuses only on gas-phase studies, because isolated, well-defined gas-phase systems are ideally suited for high-resolution experiments using state-of-the-art spectrometric and spectroscopic techniques, and for simulations employing modern quantum theoretical methods. The unmatched high complementarity and comparability of experiment and theory in the case of gas-phase investigations bear an enormous potential in providing insights in the reactions of CO_2 activation at the atomic level. In all of these examples, the reduction and bending of the inert neutral CO_2 molecule is the critical step determined by the frontier orbitals of reaction participants. Based on the results and outlook summarized in this review, we anticipate that studies of gas-phase CO_2 activations will be an avenue rich with opportunities for the rational design of novel catalysts based on the knowledge obtained on the atomic level.

Ruijing Wang obtained her master degree of science at Yantai University. Since 2021, she began her doctoral research under the direction of Professor Xinxing Zhang at Nankai University, mainly studying the electronic structures and chemical bonding of clusters using various computational methods.

Gaoxiang Liu received his B. S. in Chemistry at Fudan University in 2013. He completed his Ph.D. in Chemistry at Johns Hopkins University under the supervision of Professor Kit H. Bowen. He is currently a postdoctoral scholar at University of California, Berkeley supervised by Dr. Srigokul Upadhyayula and Dr. Eric Betzig, working on the next-generation microscopy technique for live imaging.

* Corresponding author.
E-mail address: zhangxx@nankai.edu.cn (X. Zhang).

https://doi.org/10.1016/j.jechem.2021.09.030

Seong Keun Kim received his B.Sc. in Chemistry (1980) from Seoul National University in Korea and his A.M. in Physics (1982) and Ph.D. in Chemical Physics (1987) from Harvard University. After a brief postdoctoral stint at the University of Chicago, he has been with the Chemistry Department of Seoul National University since 1989 and a former Editor-in-Chief of the journal Physical Chemistry Chemical Physics (PCCP) that covers a wide range of topics in physical chemistry. Prof. Kim himself has published papers in diverse areas of topics ranging from frequency- and time-domain spectroscopy in the gas phase and on solid surfaces, neutral and anionic clusters, nanomaterials, and single-molecule spectroscopy of biological macromolecules.

Kit H. Bowen, Jr. received his B.S. in chemistry at the University of Mississippi (1970), and his M.S. (1973) and Ph.D. (1977) in chemistry at Harvard University. He was also an NSF postdoc at Harvard University. Dr. Bowen is now the E. Emmet Reid Professor of Chemistry at the Johns Hopkins University. His research utilizes negative ion photoelectron spectroscopy and surface deposition techniques both of which are applied to size-selected cluster anions.

Xinxing Zhang, Ph.D., is a Professor of Chemistry in the College of Chemistry at Nankai University of China. Prof. Zhang earned his B.S. in chemistry at Fudan University of Shanghai in 2009, and he completed his Ph.D. in physical chemistry studying cluster mass spectrometry and laser spectroscopy in the Department of Chemistry at Johns Hopkins University under the guidance of Professor Kit Bowen in 2015. From 2016 to 2018, he performed postdoctoral research under the direction of Professor J. L. Beauchamp in the Beckman Institute of Caltech, mainly studying the oxidation and antioxidation chemistry of lipids at the air-water interface. Since 2018, he started his independent career at Nankai University through China's 1000 Talent Program. His research uses home-built apparatus to study the reaction dynamics of amphiphilic molecules at the air-water interface, as well as the laser spectroscopy and reactivity of clusters in the gas phase.

1. Introduction

It has been widely accepted that current and projected carbon dioxide (CO_2) emissions from anthropogenic activities such as the burning of fossil fuels will lead to a continued global average temperature and sea level rise [1-3]. Reducing CO_2 emission by using alternative renewable energy sources and chemically converting CO_2 into other valuable products are the two ways that promise to alleviate the current situation, but the latter does not seem to be an easy task because CO_2 is a highly stable molecule. Its high bond dissociation energy (525.9 kJ/mol [4]) and ionization potential (13.777 eV [5]) indicate that directly breaking the C-O bond or oxidizing it by taking an electron are both difficult. The carbon atom in CO_2 is in the highest oxidation state (+4), as a result, the reduction of CO_2 by electron donation might be more realistic. However, the attachment of a whole electron to CO_2 again is challenging, because CO_2 has a large highest-occupied molecular orbital (HOMO) - lowest unoccupied molecular orbital (LUMO) gap, consequently, occupying the LUMO with an electron is energetically unfavorable, which renders a negative electron affinity (-0.6 eV) [6]. As a result, CO_2 must deform to accept an electron, but the resulting bent CO_2^- anion is metastable [6-9]. Since all of these challenges are essentially caused by the intrinsic properties of CO_2 that are directly related to its molecular orbitals and the electronic structures, the investigations of the electronic structures, thermodynamics, intermediate states are vital in the deep understanding of the CO_2 activation reactions and rational designing of efficient catalysts.

Isolated and well-defined gas-phase systems are ideally suited for high-resolution experiments using state-of-the-art spectrometric and spectroscopic techniques, and for simulations employing modern quantum theoretical methods. The unmatched high complementarity and comparability of experiment and theory in the case of gas-phase investigations bear an enormous potential for investigating challenging tasks such as geometry search, intermediate capture, and chemical bonding analysis [10-16], which also provide rich opportunities in understanding the mechanistic steps in the reactions of CO_2 activation. In this review, we focus on the history, development, and outlook of isolated systems in the gas phase where CO_2 activation using single electrons, atoms, clusters, and molecules plays the key role, which we anticipate that will provide insights for the rational designing of CO_2 activation catalysts at the atomic level.

2. Activation of CO_2 with an electron

Isolated CO_2^- anion has a bent structure, where the O-C-O bond angle is 135° and the C-O bond length is increased from 1.15 Å to 1.24 Å (see Fig. 1a for the potential energy surface of CO_2^- [17]). Despite the above thermochemical arguments such as the negative electron affinity, Compton et al. have estimated a maximal lifetime of about 90 μs for the CO_2^- anion [6], as a result, experimental techniques that are faster than this timescale stand a chance of observing the metastable CO_2^- [6,18-21]. Early experiments produce CO_2^- by taking advantage of organic molecules such as cyclic anhydrides that have bent CO_2 moieties in their structures. Such experiments include the direct electron attachment to the organic molecules [18] and the collisions of the cyclic anhydrides with a cesium beam to produce the isolated bent CO_2^- product [19]. Other attempts include collisions of alkali metal atoms directly with the CO_2 molecules where the alkali metals function as electron donors to yield CO_2^- [6,20]. Remarkably, Bowen and coworkers [21] have recorded the photoelectron spectrum of CO_2^- with a 2.54 eV laser beam, which shows that the vertical detachment energy (VDE) of CO_2^- is 1.4 eV (Fig. 1b). Due to the large structural difference and the consequent poor Franck–Condon overlap between the neutral and anionic CO_2, the observed onset of the electron binding energy in Fig. 1b is much higher than the actual electron affinity (EA) of CO_2 and the whole spectrum shows a wide band. Later, Mingfei Zhou [22,23] reported the infrared spectrum of CO_2^- in solid argon matrix at 11 K. The HOMO of CO_2^- where the excess electron dwells in presented in Fig. 1c, which has π^* antibonding characteristics. The neutral and anionic CO_2 have also been extensively interrogated theoretically [24-30].

The metastable CO_2^- can be stabilized in larger clusters such as $(CO_2)_n^-$ [31-39] and $(CO_2^-)(H_2O)_n$ [40-43] as a result of the increased electron affinities (EA) and increased lifetimes. In most of the cases other than those with a $C_2O_4^-$ core (*vide infra*), the extra CO_2 or H_2O act as the "solvation" molecules for CO_2^-. The word "solvation" is the language often used in cluster science, meaning that the non-covalent interactions between the solvation molecules

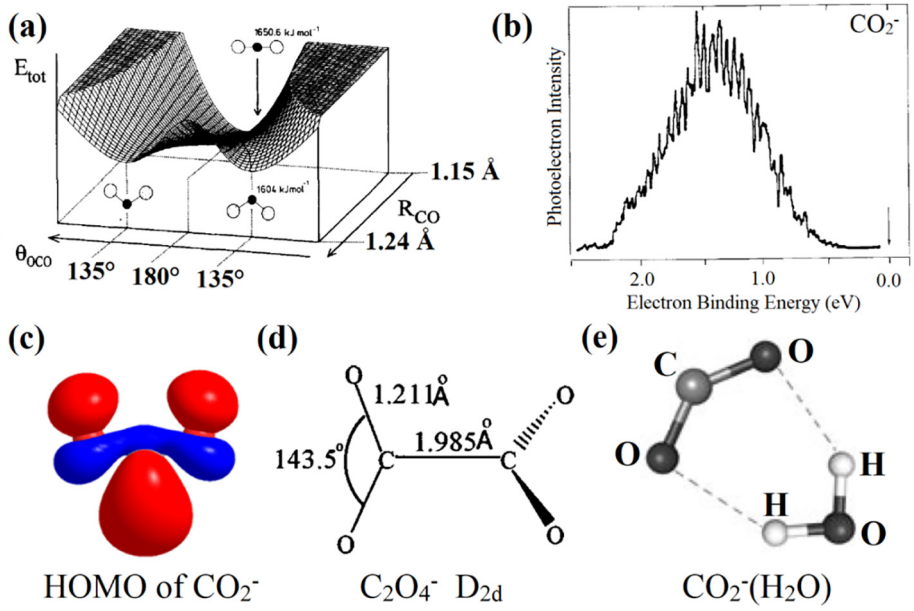

Fig. 1. (a) The potential energy surface of CO_2^-. Reproduced from Ref. [17]. (b) The photoelectron spectrum of CO_2^-. Reproduced from Ref. [21] with permission from Springer Nature. (c) The HOMO of CO_2^-, (d) the structure of $C_2O_4^-$. Reproduced from Ref. [22] with permission from AIP Publishing, and (e) the structure of CO_2^- (H_2O). Reproduced from Ref. [43] with permission from Wiley-VCH.

and the core anions lower the energy of the anion more than the corresponding neutral, yielding increased EAs. Klots and Compton first generated $(CO_2)_n^-$ clusters with electron attachment to a supersonic neutral CO_2 beam [22,31], after which people realized that the anionic core of these clusters could be either CO_2^- or $C_2O_4^-$ (Fig. 1d). Anion photoelectron spectroscopy [33,34], infrared spectroscopy [35], photoelectron angular distribution imaging [36] techniques, as well as theoretical studies [37-39] have revealed that the core is switching between CO_2^- and $C_2O_4^-$ at different cluster sizes. Water is apparently another good solvation molecule for CO_2^-, and Klots [40] reported that just one water molecule is sufficient to prevent electron autodetachment in CO_2^- (H_2O). Later, bigger clusters $(CO_2^-)(H_2O)_n$ were investigated both experimentally and theoretically [41-43] (Fig. 1e).

3. Activation of CO_2 with a metal atom

The interaction of CO_2 with a metal atom can be regarded as a simplified model of atomically rough surfaces with metal atoms that are not fully coordinated, and these corner or edge sites are considered as the major active moieties of catalytic CO_2 activation

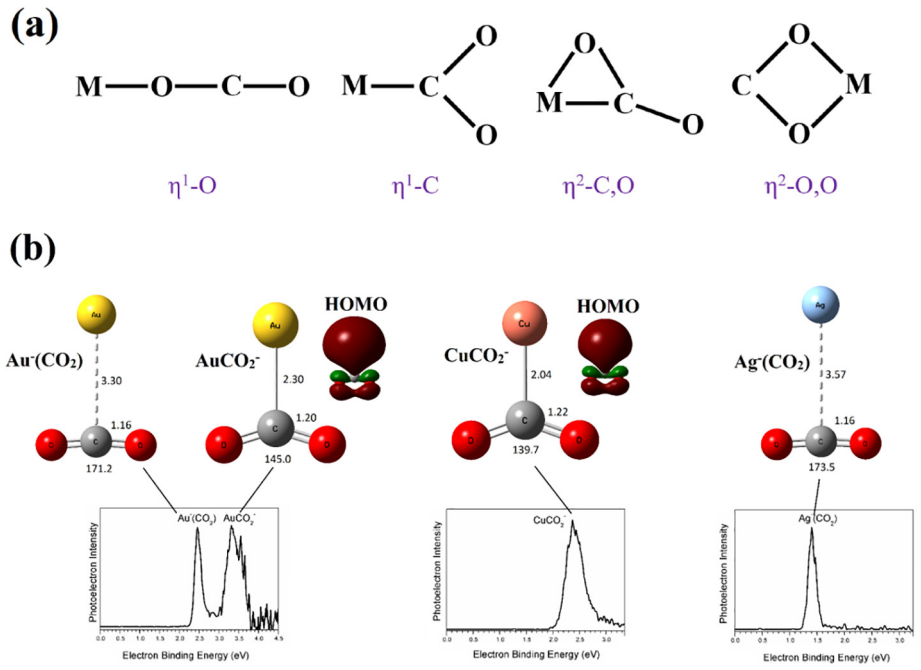

Fig. 2. (a) The four ways that a metal M interacts with CO_2, (b) the structures, HOMO, and anion photoelectron spectra of $(M\text{-}CO_2)^-$ (M = Cu^-, Ag^-, Au^-). Reproduced from Ref. [55] with permission from AIP Publishing.

on materials. In the gas phase, CO_2 and an atom will bind in one of the four forms depicted in Fig. 2a, they being η^1-O, η^1-C, η^2-C, O and η^2-O, O, where the superscripted numbers denote the number of coordination to the metal center. For the η^1-O cases, previous studies from Duncan and Mackenzie groups using ion beam and infrared photodissociation techniques include V^+, Si^+, Ni^+, Mg^+, Fe^+, Al^+, Ca^+, Co^+, Rh^+, and Ir^+, all of which follow the M^+–O = C = O configuration [44-52], where CO_2 acts as weakly-bound solvation molecules and is slightly positively charged. Three exceptions were also found: in the case of $V^+(CO_2)_n$, charge transfer occurs in larger clusters and yields the $V^{2+}(CO_2)_{n-2}(C_2O_4^-)$ cluster [44]; in the cases of $Si^+(CO_2)_n$ and $Ni^+(CO_2)_n$, the Si or Ni center inserts into a C-O bond of a CO_2 molecule, forming O-M-CO oxide-carbonyl products [45,46]. Armentrout and Schwarz groups summarized the thermodynamics of cationic metal-CO_2 interactions [53,54].

The η^1-C and the η^2-C,O scenarios have more charge transfer from the center atom to CO_2. Using mass spectrometric and anion photoelectron spectroscopic methods, Zhang, Liu and Bowen investigated the interactions between Cu^-, Ag^-, Au^-, Ni^-, Pd^-, Pt^- and CO_2 [55-57]. All of the six examples follow the η^1-C structure with subtle differences among them. They discovered that in $(M\text{-}CO_2)^-$ (M = Cu^-, Ni^-, Pd^-, Pt^-), the interaction between the metal center and CO_2 is strong (chemisorption), forming formate-like anions (metalloformates), the excess electron occupying the HOMO is delocalized in all the four atoms, and the CO_2 moiety is negatively charged up to −0.64 *e* (Fig. 2b). Nevertheless, in $(Ag\text{-}CO_2)^-$, the interaction between the metal and CO_2 is weak (physisorption), and CO_2 acts as a solvation molecule [denoted as $Ag^-(CO_2)$], resulting in little charge transfer to CO_2 (Fig. 2b). The $(Au\text{-}CO_2)^-$ cluster surprisingly has both of the chemisorbed and physisorbed isomers denoted as $AuCO_2^-$ and $Au^-(CO_2)$, respectively (Fig. 2b). Even though it is still enigmatic why these three coinage metal atomic anions behave so differently in activating CO_2, these results have brought new insights in understanding the catalytic efficiency when using related materials. Kim and coworkers [57] rationalized the η^1-C activation using M_n^- (M = Cu, Ag, Au) with the analyses of the symmetries of the frontier orbitals. For *n* = 1, 2, 6, the HOMO of M_n^- presents an s-type orbital of the metals, which matches the symmetry of the LUMO of CO_2. As a result, the doubly occupied HOMO of M_n^- can be inserted into the empty LUMO of CO_2 to produce a bond is similar to a dative bond, resulting in the bending and activation of CO_2. This work has pointed out a promising way of activating CO_2 by analyzing the symmetry of the frontier orbitals of the catalyst. Weber's group also studied the activation of CO_2 with Cu^-, Ag^-, Au^-, Bi^-, Fe^-, Co^- and Ni^- using infrared spectroscopy [58-64]. Remarkably, in $Bi(CO_2)_n^-$, they observed the formation of the $C_2O_4^{2-}$ (oxalate) moiety [61], in $Fe(CO_2)_n^-$ they observed the η^2-C, O structure, oxalate, and O- M-CO (oxide-carbonyl) products simultaneously [62], and in the $Co(CO_2)_n^-$ case they discovered that the core is a Co^+ metal center binding with two highly negatively charged CO_2 molecules in the η^2-C,O manner [63]. Finally, the η^2-O,O structures were mainly found between neutral alkali metal atoms and CO_2 characterized by infrared spectroscopy in low-temperature frozen insert gas matrices, where the CO_2 moieties are all significantly reduced [65-67].

Recently, scientists are observing a new era of single-atom catalysis and atom economy, which emphasizes the fact that the ultimate small-size limit for metal particles is one atom [68,69]. SACs on supports are not fully coordinated, and the vacant sites are often catalytically active sites, similar to the "naked" single atom catalysts in gas-phase studies. In addition, SACs are usually charged due to the electron density transfer between the support and the catalyst, which can also be recovered by the charged atomic ions in the gas phase. More importantly, the much simpler model systems in the gas phase facilitates straightforward experimental and theoretical investigations of the frontier orbitals involved in the reactions, which might also be parallel to the active molecular orbitals in the SAC studies. Therefore, we anticipate that this summary of isolated single atom in the gas phase for the activation of CO_2 will bring new atomic-level insights for the design of novel catalysts with high activity and specificity.

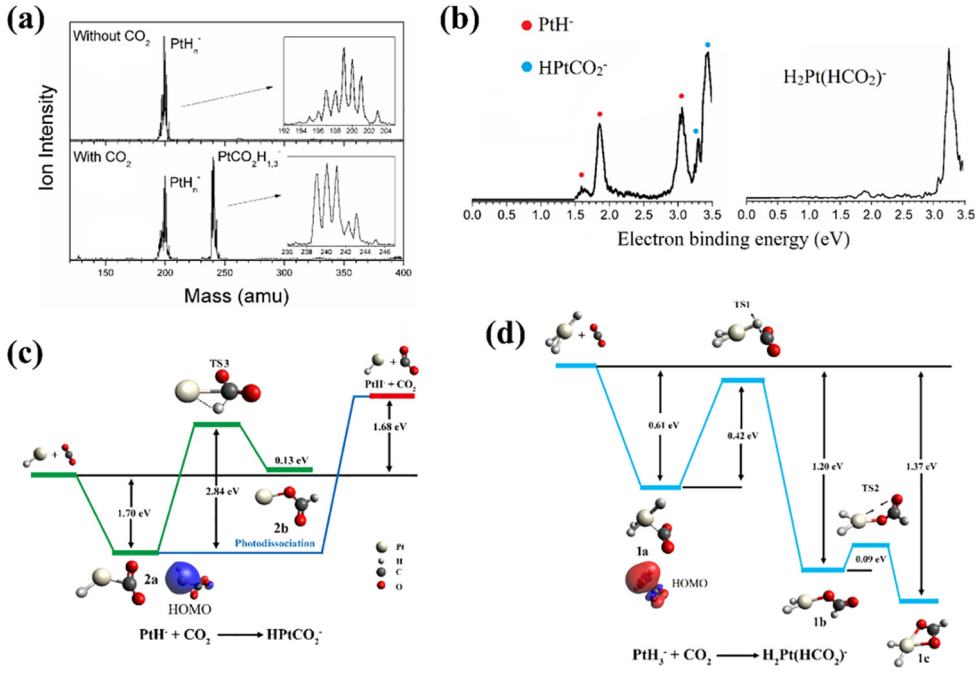

Fig. 3. (a) The mass spectra showing the reaction between PtH_n^- and CO_2, (b) the anion photoelectron spectra of the products in (a), (c) the calculated potential energy surface of the reaction between PtH^- and CO_2, (d) the calculated potential energy surface of the reaction between PtH_3^- and CO_2. Reproduced from Ref. [72] with permission from Wiley-VCH.

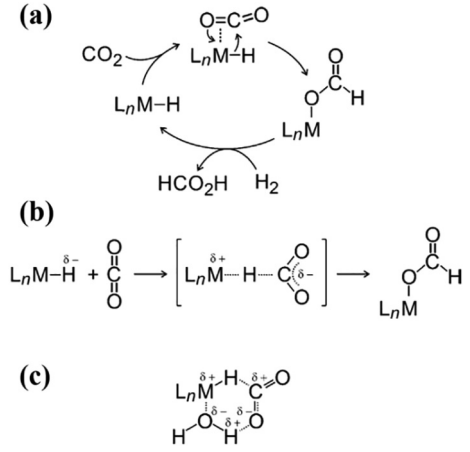

Fig. 4. The three potential mechanistic pathways of CO_2 hydrogenation using metal hydrides summarized by Schwarz. Reproduced from Ref. [54].

4. Activation of CO_2 with a cluster

As a bridge connecting single atoms and real materials, gas-phase clusters represent ideal model systems to gain molecular-level insights into the energetics and kinetics of catalytic reactions [70,71]. In this section, we focus on the examples of CO_2 activation using gas-phase metal hydride clusters, because hydrogenation of CO_2 often results in value-added products such as formate or methanol. CO_2 activation using clusters including metal hydrides was summarized in a review article from Schwarz group [54].

On the technical front, gas phase cluster-CO_2 reactions have been performed in flow tube, linear ion trap, and Fourier transform ion-cyclotron resonance cell. The resulting products are characterized by mass spectrometry, anion photoelectron spectroscopy, collision-induced dissociation and infrared action spectroscopy methodologies [72-85]. Such hydride clusters include PtH_n^- [72], $PdCuH_n^-$ [73], PdH_n^- [74], $LTiH^+$ (L = ligand) [75], $Cu_xH_y^-$ [76,77], $Fe_xH_y^-$ [78,79], CoH^-/NiH^-/CuH^- [80], LAg_2H^+ (L = ligand) [81], and $ScNH^+$ [82].

Taking the reactions between PtH_n^- and CO_2 as an example [72], the mass spectra with or without CO_2 pulsed into the reaction cell are shown in Fig. 3a. With no CO_2, only PtH_n^- cluster anions were observed in the mass spectrum. By recording anion photoelectron spectra at every mass peak in the series of PtH_n^- species, the authors confirmed that species with n = 1, 2, 3, 5 were present. When CO_2 was added to the cell, the ion intensity of the PtH_n^- series decreased, and a new series of $PtCO_2H_m^-$ cluster anions appeared. Again by taking the photoelectron spectra of the $PtCO_2H_m^-$ series, $PtCO_2H^-$ and $PtCO_2H_3^-$ were found to be the only reaction products, whose structures were confirm by the comparison of the calculated transition energies and the recorded spectra (Fig. 3b). The spectral features of $PtCO_2H^-$ are due not only to the photodetachment of $PtCO_2H^-$, but also to the photodissociation of $PtCO_2H^-$ into PtH^- and CO_2, followed by photodetachment of the resultant PtH^- anion. The latter is a two-photon process inducing photodissociation and photodetachment of the anionic product of photodissociation. This remarkable observation is in line with the calculated structure of $PtCO_2H^-$ where the CO_2 moeity still exists and binds with the PtH^- part in the η^2-C,O manner (Fig. 3c). Fig. 3c presents the potential energy pathway for the reaction between CO_2 and PtH^-. In the first step, CO_2 is activated through charge transfer from the Pt atom, forming Pt-C and Pt-O bonds. Its HOMO shows substantial delocalization, manifesting the charge transfer from Pt to CO_2. The activation of CO_2 provides 1.70 eV of stabilization energy for $PtCO_2H^-$. Nevertheless, even though CO_2 activation has been achieved at this point, the reaction cannot proceed further to CO_2 hydrogenation due to the 2.84 eV energy barrier. The pathway of CO_2 hydrogenation by PtH_3^- is presented in Fig. 3d. PtH_3^- exhibits C_{2v} symmetry. The first step in the reaction is again the CO_2 activation through charge transfer from PtH_3^-. As soon as CO_2 approaches the Pt atom, it bends, and the C atom in CO_2 attaches to Pt in the η^1-C manner with an energy drops of 0.61 eV in the first step. The HOMO of the PtH_3CO_2 structure with the activated CO_2 shows that the excess electron is also delocalized over the entire cluster. Natural population analysis calculation shows that the net charge on the CO_2 moiety is −0.39 *e*. After activation, the CO_2 moiety is ready to accept an H atom from PtH_3^-. The insertion of CO_2 into the Pt-H bond passes through the first transition state with an energy barrier of 0.42 eV. Once the hydrogen atom has transferred to CO_2, hydrogenation is complete, yielding a local minima. In order for $PtCO_2H_3^-$ to reach the global minimum structure, i.e., to reach the final structure in Fig. 3d, the local minima must surmount a second transition state that allows the other O atom to coordinate with the Pt atom, further stabilizing the entire cluster, yielding the final $H_2Pt(HCO_2)^-$ product.

Schwarz in his review article [54] summarized the three potential mechanistic pathways of CO_2 hydrogenation using metal hydrides in the gas phase(Fig. 4 where L denotes ligands). (a) The η^2-C,O coordination of CO_2 to an empty site of the metal core is followed by a hydride transfer to yield the formate ligand, and the latter is eventually cleaved from the metal by hydrogenation to regenerate the catalyst L_nMH. The example in Fig. 3 partially follows this mechanism. (b) The η^1-C coordination of CO_2 to the hydrogen atom in L_nMH, followed by a hydride shift. (c) Water promotes the hydride transfer through a network of hydrogen bonding to the incoming CO_2 ligand. All CO_2 hydrogenation reactions more or less follow these three scenarios.

The above example indicates that the activation and hydrogenation of CO_2 by gas phase clusters highly depend on the energetics of the reaction pathways. Calculations often play an indispensable role in the understanding of the experimental results, searching for the transition states, and visualization of the molecular orbitals that are directly involved in the reactions. These results again emphasize the high complementarity and comparability of experiment and theory in gas-phase investigations, which is advantageous in providing the detailed insights of the catalytic pathways. It is worth mentioning that gas-phase hydrogenation often uses clusters that are not fully coordinated. Bulk reactions usually utilize saturated metal hydride complexes. As a result, the catalytic cycle in the bulk involves the loss of a ligand, resulting in an active vacant site for the CO_2 activation [83,84]. This particular step is similar to the gas-phase scenarios. After CO_2 activation, the uncoordinated sites could be soon be refilled by a ligand in the solution. Therefore, the gas-phase study might be viewed as a critical mechanistic step in a complete catalytic cycle.

5. Activation of CO_2 with a molecule

The activation of small molecules often involves expensive transition metal catalysts. From economic considerations, the utilization of inexpensive, non-metal molecules in activating CO_2 seems to be in need. In 2000, Kim and coworkers [85] discovered that by the electron attachment to CO_2 and pyridine (Py), a N-heterocycle (NHC) molecule, they could make a stable planar anionic complex $(Py\text{-}CO_2)^-$, in which the CO_2 moiety is bent and negatively charged by −0.5 *e* (Fig. 5a). The complex was characterized by gas-phase anion photoelectron spectroscopy, which revealed high vertical detachment energy of the product. Calculations showed a π bond network throughout the whole molecule. Since both CO_2 and Py have negative electron affinities, the fact that their

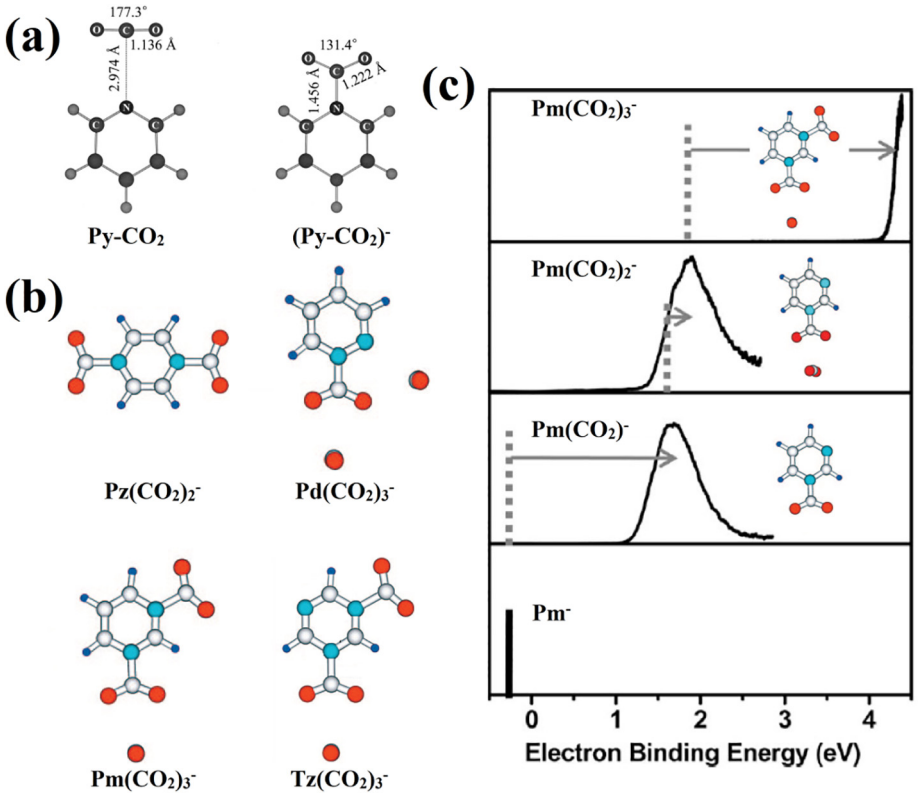

Fig. 5. (a) The structures of neutral and anionic Py-CO_2. Reproduced from Ref. [85] with permission from AIP Publishing. (b) The structures of anionic $Pz(CO_2)^-_2$, $Pd(CO_2)^-_3$, $Pm(CO_2)^-_3$ and $Tz(CO_2)^-_3$. Reproduced from Ref. [87] with permission from the American Chemical Society, and (c) anion photoelectron spectral shift as an indicator for the bonding situation of CO_2 using $Pm(CO_2)_n^-$ as an example. Reproduced from Ref. [87] with permission from the American Chemical Society.

anionic complex can form at all was initially surprising. A reasonable explanation for this would be that the extended π-conjugated system over the entire complex allows the accommodation of the extra electron. Later, Johnson and coworkers [86] studied the same system using gas-phase infrared photodissociation techniques. Further, Kim's group [87] extended the studies to several other azabenzene NHC molecules including pyridazine (1,2-diazine, Pd), pyrimidine (1,3-diazine, Pm), pyrazine (1,4-diazine, Pz), as well as s-triazine (1,3,5-triazine, Tz). They discovered that Pz accommodated a maximum of two CO_2 molecules, Pd accommodated one, Pm accommodated two, and Tz accommodated two CO_2 molecules (Fig. 5b). Interestingly, CO_2 molecules do not add to the N atoms of the NHC molecules sequentially. Taking the Pm $(CO_2)_n^-$ system as an example (Fig. 5c), the attachment of the electron and the first CO_2 molecule significantly increases the electron vertical detachment energy, suggesting a substantial structural change in the chromophore for the electron photodetachment, and this is due to the C-N bond formation between CO_2 and Pm, resulting in an anion complex similar to the $(Py\text{-}CO_2)^-$ in Fig. 5a. However, the addition of a second CO_2 only slightly blue shifts the spectrum, indicating that the second CO_2 molecule acts as a solvation molecule. The introduction of a third CO_2 again drastically shifts the spectrum, which is in line with a second C-N bond formation between CO_2 and Pm. The uptake of CO_2 molecules by these NHC azabenzenes apparently is influenced by both of the steric hindrance and energy released upon forming the complexes. In 2015, Bowen's group [88] extended the work to another NHC molecule quinoline using anion photoelectron spectroscopy methods and discovered similar structures and spectral features. The lone pairs on these heterocycles obviously play critical roles on the CO_2 activation, whose symmetry matches the LUMO of CO_2, similar to the cases of the and the η^1-C activation using M_n^- (M = Cu, Ag, Au) [57]. The resultant delocalized molecular orbital on the whole product is apparently another reason that rationalizes the formation of the counterintuitive product.

The CO_2 activation efficiency of these systems can be rationalized by the electron affinities (EA) of both of the products and the catalysts. Taking the above organic bases (NHC) activated CO_2 reactions as an example, the high electron affinity stemming from the π-orbital delocalization in the final product, $(NHC\text{-}CO_2)^-$, renders a thermodynamically-favored reaction pathway, as a result, the higher EA of the final product promises a more efficient CO_2 reduction rate [85-88]. In a more recent study, Toma and coworkers [89] utilized pyridine-substituted cobalt (II) phthalocyanine to catalyze the electrochemical reduction of CO_2. They find that the introduction of the pyridine moiety increases the EA of the catalyst and enhances the CO_2 conversion rate. It is postulated that the electron uptake by the catalyst is a key step in determining the overall reaction efficiency, hence, a higher EA renders a thermodynamically-favored reduction of the catalyst, resulting in an overall enhanced CO_2 reduction rate.

Similar bonding situations as the NHC cases have also been observed in the condensed phase, where neural complexes were formed between lone pairs of electrons and CO_2. Schossler and Regitz [90] first synthesized neutral complexes between N-heterocyclic carbenes (NHCars) and CO_2, with a covalent C–C bond in the NHCar-CO_2 product. Other examples [91-94] also observed a bent CO_2 moiety with a significant negative charge in several $(NHCar\text{-}CO_2)$ complexes. Despite being neural, carbene's high-lying HOMO allows NHCars to donate electron density to the LUMO of CO_2, making the product with a charge-separated configuration i.e., $NHCar^+–CO_2^-$. Later, the unique $(NHCar\text{-}CO_2)$ complexes were further applied to CO_2 capture and reduction [95-99]. More recently, ionic liquids have also been extensively studied in the

applications of CO_2 activation, where the lone electron pairs on the cationic part of the ionic liquid play similar roles as the above NHCars in activating CO_2 molecules [100,101].

6. Conclusions and perspectives

The gas-phase CO_2 activation studies using electrons, atoms, clusters or molecules summarized in this review can be generally regarded as model systems that represent the intermediates in the solid-state CO_2 activation and conversion, and bring atomic-level insights for the mechanisms of these reactions. Even though in the past decades the topic of CO_2 conversion have been extensively studied, the capture and characterization of these elusive intermediates that bear key mechanistic information remain difficult, mainly due to the fact that these species often have short lifetime and unstable nature. Isolated *in-vacuo* gas-phase studies equipped with state-of-the-art spectrometric and spectroscopic methods fit right into the void of investigating this topic, and theoretical calculations also play indispensable roles in understanding the experimental results and predicting potential reaction pathways. We anticipate that studies of gas-phase CO_2 activations combined with quantum chemical calculations will be an avenue rich with opportunities for the rational design of novel catalysts based on the knowledge obtained on the atomic level.

Declaration of Competing Interest

The authors declare that they have no known competing financial interests or personal relationships that could have appeared to influence the work reported in this paper.

Acknowledgments

X.Z. acknowledges the National Key R&D Program of China (2018YFE0115000), the National Natural Science Foundation of China (22003027 and 22174073), the NSF of Tianjin City (19JCYBJC19600) and the Frontiers Science Center for New Organic Matter of Nankai University (63181206). Some of the experiments described in this work were supported by the Air Force Office of Scientific Research (AFOSR) under grant number, FA9550-19-1-0077 (KHB).

References

[1] P.T. Brown, K. Caldeira, Nature. 552 (2017) 45–50.
[2] P.M. Cox, R.A. Betts, C.D. Jones, S.A. Spall, I.J. Totterdell, Nature. 408 (2000) 184–187.
[3] F. Joos, G.K. Plattner, T.F. Stocker, O. Marchal, A. Schmittner, Science. 284 (1999) 464–467.
[4] B.dB. Darwent, Bond Dissociation Energies in Simple Molecules, Natl. Stand. Ref. Data Ser, Natl. Bur. Stand. 31, Washington, 1970.
[5] S.G. Lias, "Ionization Energy Evaluation" in NIST Chemistry WebBook, NIST Standard Reference Database Number 69, National Institute of Standards and Technology, Gaithersburg MD, 2017.
[6] R.N. Compton, P.W. Reinhardt, C.D. Cooper, J. Chem. Phys. 63 (1975) 3821.
[7] S.H. Fleischman, K.D. Jordan, J. Phys. Chem. 91 (1987) 1300–1302.
[8] D. Yu, A. Rauk, D.A. Armstrong, J. Phys. Chem. 96 (1992) 6031–6038.
[9] A. Stamatovic, K. Leiter, W. Ritter, K. Stephan, T.D. Mark, J. Chem. Phys. 83 (1985) 2942–2946.
[10] A.W. Castleman, R.G. Keesee, Science. 241 (1988) 36–42.
[11] X. Zhang, I.A. Popov, K.A. Lundell, H. Wang, C. Mu, W. Wang, H. Schnockel, A.I. Boldyrev, K.H. Bowen, Angew. Chem. Int. Ed. 57 (2018) 14060–14064.
[12] X. Zhang, G.X. Liu, S. Ciborowski, W. Wang, C. Gong, Y.F. Yao, K.H. Bowen, Angew. Chem. Int. Ed. 58 (2019) 11400–11403.
[13] G.X. Liu, N. Fedik, C. Martinez-Martinez, S.M. Ciborowski, X. Zhang, A.I. Boldyrev, K.H. Bowen, Angew. Chem. Int. Ed. 58 (2019) 13789–13793.
[14] W. Wang, M. Marshall, E. Collins, S. Marquez, C. Mu, K.H. Bowen, X. Zhang, Nat. Commun. 10 (2019) 1170–1176.
[15] X. Zhang, G.X. Liu, S. Ciborowski, K.H. Bowen, Angew. Chem. Int. Ed. 56 (2017) 9897–9900.
[16] D.K. Böhme, H. Schwarz, Angew. Chem. Int. Ed. 44 (2005) 2336–2354.
[17] H.J. Freund, M.W. Roberts, Surf. Sci. Rep. 25 (1996) 225–273.
[18] C.D. Cooper, R.N. Compton, J. Chem. Phys. 59 (1973) 3550–3565.
[19] C.D. Cooper, R.N. Compton, Chem. Phys. Lett. 14 (1972) 29–32.
[20] S.Y. Tang, E.W. Rothe, G.P. Reck, J. Chem. Phys. 61 (1974) 2592–2595.
[21] K.H. Bowen, J.G. Eaton, in: The Structure of Small Molecules and Ions, Springer US, Boston, MA, 1989, pp. 147–169.
[22] M.F. Zhou, L. Andrews, J. Chem. Phys. 110 (1999) 2414–2422.
[23] M.F. Zhou, L. Andrews, J. Chem. Phys. 110 (1999) 6820–6826.
[24] J. Pacansky, U. Wahlgren, P.S. Bagus, J. Chem. Phys. 62 (1975) 2740–2744.
[25] P.J. Bruna, S.D. Peyerimhoff, Chem. Phys. Lett. 39 (1976) 211–216.
[26] T. Sommerfeld, H.D. Meyer, L.S. Cederbaum, Phys. Chem. Chem. Phys. 6 (2004) 42–45.
[27] G.L. Gutsev, R.J. Bartlett, R.N. Compton, J. Chem. Phys. 108 (1998) 6756–6762.
[28] A.R. Rossi, K.D. Jordan, J. Chem. Phys. 70 (1979) 4422–4424.
[29] M. Saeki, T. Tsukuda, T. Nagata, Chem. Phys. Lett. 348 (2001) 461–468.
[30] M. Krauss, D. Neumann, Chem. Phys. Lett. 14 (1972) 26–28.
[31] C.E. Klots, R.N. Compton, J. Chem. Phys. 67 (1977) 1779–1780.
[32] C.E. Klots, R.N. Compton, J. Chem. Phys. 69 (1978) 1636–1643.
[33] M.J. DeLuca, B. Niu, M.A. Johnson, J. Chem. Phys. 88 (1988) 5857–5863.
[34] T. Tsukuda, M.A. Johnson, T. Nagata, Chem. Phys. Lett. 268 (1997) 429–433.
[35] J.W. Shin, N.I. Hammer, M.A. Johnson, H. Schneider, A. Glo1â, J.M. Weber, J. Phys. Chem. A 109 (2005) 3146–3152.
[36] R. Mabbs, E. Surber, L. Velarde, A. Sanov, J. Chem. Phys. 120 (2004) 5148–5154.
[37] M. Saeki, T. Tsukuda, T. Nagata, Chem. Phys. Lett. 340 (2001) 376–384.
[38] T. Sommerfeld, T. Posset, J. Chem. Phys. 119 (2003) 7714–7724.
[39] M. Kondo, T. Takayanagi, Comput Theor. Chem. 1105 (2017) 61–68.
[40] C.E. Klots J. Chem. Phys. 71 (1979) 4172–4172.
[41] T. Tsukuda, M. Saeki, R. Kimura, T. Nagata, J. Chem. Phys. 110 (1999) 7846–7857.
[42] M. Saeki, T. Tsukuda, S. Iwata, T. Nagata, J. Chem. Phys. 111 (1999) 6333–6344.
[43] O.P. Balaj, C.K. Siu, I. Balteanu, M.K. Beyer, V.E. Bondybey, Chem. Eur. J. 10 (2004) 4822–4830.
[44] A.M. Ricks, A.D. Brathwaite, M.A. Duncan, J. Phys. Chem. A 117 (2013) 11490–11498.
[45] J.B. Jaeger, T.D. Jaeger, N.R. Brinkmann, H.F. Schaefer, M.A. Duncan, Can. J. Chem. 82 (2004) 934–946.
[46] N.R. Walker, R.S. Walters, G.A. Grieves, M.A. Duncan, J. Chem. Phys. 121 (2004) 10498–10507.
[47] N.R. Walker, R.S. Walters, M.A. Duncan, J. Chem. Phys. 120 (2004) 10037–10045.
[48] G. Gregoire, J. Velasquez, M.A. Duncan, Chem. Phys. Lett. 349 (2001) 451–457.
[49] G. Gregoire, M.A. Duncan, J. Chem. Phys. 117 (2002) 2120–2130.
[50] R.S. Walters, N.R. Brinkmann, H.F. Schaefer, M.A. Duncan, J. Phys. Chem. A 107 (2003) 7396–7405.
[51] C.T. Scurlock, S.H. Pullins, M.A. Duncan, J. Chem. Phys. 105 (1996) 3579–3585.
[52] A. Iskra, A.S. Gentleman, A. Kartouzian, M.J. Kent, A.P. Sharp, S.R. Mackenzie, J. Phys. Chem. A 121 (2017) 133–140.
[53] P.B. Armentrout, Annu. Rev. Phys. Chem. 52 (2001) 423–461.
[54] H. Schwarz, Coord. Chem. Rev. 334 (2017) 112–123.
[55] X. Zhang, E. Lim, S.K. Kim, K.H. Bowen, J. Chem. Phys. 143 (2015) 174305–174310.
[56] G.X. Liu, S.M. Ciborowski, Z.G. Zhu, Y.L. Chen, X. Zhang, K.H. Bowen, Phys. Chem. Chem. Phys. 21 (2019) 10955–10960.
[57] E. Lim, J. Heo, X. Zhang, K.H. Bowen, S.H. Lee, S.K. Kim, J. Phys. Chem. A 125 (2021) 2243–2248.
[58] B.J. Knurr, J.M. Weber, J. Am. Chem. Soc. 134 (2012) 18804–18808.
[59] B.J. Knurr, J.M. Weber, J. Phys. Chem. A 117 (2013) 10764–10771.
[60] B.J. Knurr, J.M. Weber, J. Phys. Chem. A 118 (2014) 10246–10251.
[61] M.C. Thompson, J. Ramsay, J.M. Weber, Angew. Chem. Int. Ed. 55 (2016) 15171–15174.
[62] M.C. Thompson, L.G. Dodson, J.M. Weber, J. Phys. Chem. A 121 (2017) 4132–4138.
[63] B.J. Knurr, J.M. Weber, J. Phys. Chem. A 118 (2014) 4056–4062.
[64] B.J. Knurr, J.M. Weber, J. Phys. Chem. A 118 (2014) 8753–8757.
[65] Z.H. Kafafi, R.H. Hauge, W.E. Billups, J.L. Margrave, Inorg. Chem. 23 (1984) 177–183.
[66] L. Manceron, A. Loutellier, J.P. Perchard, J. Mol. Struct. 129 (1985) 115–124.
[67] V.N. Solov'ev, E.V. Polikarpov, A.V. Nemukhin, G.B. Sergeev, J. Phys. Chem. A 103 (1999) 6721–6725.
[68] A.Q. Wang, J. Li, T. Zhang, Nat. Rev. Chem. 2 (2018) 65–81.
[69] X.F. Yang, A.Q. Wang, B.T. Qiao, J. Li, J.Y. Liu, T. Zhang, Acc. Chem. Res. 46 (2013) 1740–1748.
[70] D.J. Harding, A. Fielicke, Chem. Eur. J. 20 (2014) 3258–3267.
[71] S.M. Lang, T.M. Bernhardt, Phys. Chem. Chem. Phys. 14 (2012) 9255–9269.
[72] X. Zhang, G.X. Liu, K.H. Meiwes-Broer, G. Ganteför, K.H. Bowen, Angew. Chem. Int. Ed. 55 (2016) 9644–9647.
[73] G.X. Liu, P. Poths, X. Zhang, Z.G. Zhu, M. Marshall, M. Blankenhorn, A.N. Alexandrova, K.H. Bowen, J. Am. Chem. Soc. 142 (2020) 7930–7936.
[74] G.X. Liu, Z.G. Zhu, M. Marshall, M. Blankenhorn, K.H. Bowen, J. Phys. Chem. A 125 (2021) 1747–1753.
[75] S.Y. Tang, N.J. Rijs, J.L. Li, M. Schlangen, H. Schwarz, Chem. Eur. J. 21 (2015) 8483–8490.
[76] A. Zavras, H. Ghari, A. Ariafard, A.J. Canty, Inorg. Chem. 56 (2017) 2387–2399.
[77] Y.Z. Liu, L.X. Jiang, X.N. Li, L.N. Wang, J.J. Chen, S.G. He, J. Phys. Chem. C 122 (2018) 19379–19384.

[78] L.X. Jiang, C.Y. Zhao, X.N. Li, H. Chen, S.G. He, Angew. Chem. Int. Ed. 56 (2017) 4187–4191.
[79] Y.Z. Liu, X.N. Li, S.G. He, J. Phys. Chem. A 124 (2020) 8414–8420.
[80] L.X. Jiang, X.N. Li, S.G. He, J. Phys. Chem. C 124 (2020) 5928–5933.
[81] A. Zavras, G.N. Khairallah, M. Krstić, M. Girod, S. Daly, R. Antoine, P. Maitre, R. J. Mulder, S.A. Alexander, V. Bonačić-Koutecký, P. Dugourd, R.A.J. O'Hair, Nat. Commun. 7 (2016) 11746–11748.
[82] M. Wang, C.X. Sun, J.T. Cui, Y.H. Zhang, J.B. Ma, J. Phys. Chem. A 123 (2019) 5762–5767.
[83] G.J. Xia, J. Liu, Z.F. Liu, Phys. Chem. Chem. Phys. 21 (2019) 19252–19268.
[84] Y.Y. Ohnishi, T. Matsunaga, Y. Nakao, H. Sato, S. Sakaki, J. Am. Chem. Soc. 127 (2005) 4021–4032.
[85] S.Y. Han, I. Chu, J.H. Kim, J.K. Song, S.K. Kim, J. Chem. Phys. 113 (2000) 596–601.
[86] M.Z. Kamrath, R.A. Relph, M.A. Johnson, J. Am. Chem. Soc. 132 (2010) 15508–15511.
[87] S.H. Lee, N. Kim, D.G. Ha, S.K. Kim, J. Am. Chem. Soc. 130 (2008) 16241–16244.
[88] J.D. Graham, A.M. Buytendyk, Y. Wang, S.K. Kim, K.H. Bowen, J. Chem. Phys. 142 (2015) 234307–234310.
[89] A.D. Riccardis, M. Lee, R.V. Kazantsev, A.J. Garza, G. Zeng, D.M. Larson, E.L. Clark, P. Lobaccaro, P.W.W. Burroughs, E. Bloise, J.W. Ager, A.T. Bell, M. Head-Gordon, G. Mele, F.M. Toma, A.C.S. Appl, Mater. Interfaces. 12 (2020) 5251–5258.
[90] W. Schossler, M. Regitz, Chem. Ber. 107 (1974) 1931–1948.
[91] N. Kuhn, M. Steimann, G. Weyers, Z.B. Naturforsch, J. Chem. Sci. 54 (1999) 427–433.
[92] H.A. Duong, T.N. Tekavec, A.M. Arif, J. Louie, Chem. Commun. (2004) 112–113.
[93] B.R. Van Ausdall, J.L. Glass, K.M. Wiggins, A.M. Aarif, J. Louie, J. Org. Chem. 74 (2009) 7935–7942.
[94] M. Vogt, J.E. Bennett, Y. Huang, C. Wu, W.F. Schneider, J.F. Brennecke, B.L. Ashfeld, Chem. Eur. J. 19 (2013) 11134–11138.
[95] L. Yang, H. Wang, ChemSusChem 7 (2014) 962–998.
[96] F. Huang, G. Lu, L.L. Zhao, H.X. Li, Z.X. Wang, J. Am. Chem. Soc. 132 (2010) 12388–12398.
[97] H. Zhou, W.Z. Zhang, C.H. Liu, J.P. Qu, X.B. Lu, J. Org. Chem. 73 (2008) 8039–8044.
[98] W.Y. Li, D.F. Huang, Y.J. Lv, RSC Adv. 4 (2014) 17236–17244.
[99] S.N. Riduan, Y.Z. Zhang, J.Y. Ying, Angew. Chem. Int. Ed. 48 (2009) 3322–3325.
[100] B.A. Rosen, A. Salehi-Khojin, M.R. Thorson, W. Zhu, D.T. Whipple, P.J.A. Kenis, R.I. Masel, Science. 334 (2011) 643–644.
[101] S.J. Zeng, X.P. Zhang, L. Bai, X.C. Zhang, H. Wang, J.J. Wang, D. Bao, M.D. Li, X.Y. Liu, S.J. Zhang, Chem. Rev. 117 (2017) 9625–9673.